International Journal of Mass Spectrometry 306 (2011) iv–ix

Contents lists available at ScienceDirect

International Journal of Mass Spectrometry

journal homepage: www.elsevier.com/locate/ijms

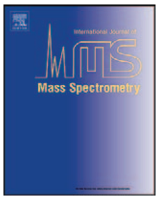

Contents

Foreword

Curriculum Vitae

Personal Foreword

Elsevier B.V.
doi:10.1016/S1387-3806(11)00342-3

Regular articles

99–107

Amplified histidine effect in electron-transfer dissociation of histidine-rich peptides from histatin 5

Thomas W. Chung, František Tureček

▶ ETD of histidine-rich peptides provides complete sequence coverage. ▶ Charge-reduced survivor ions undergo specific rearrangements. ▶ Multi-stage CID reveals the histidine rearrangement sites.

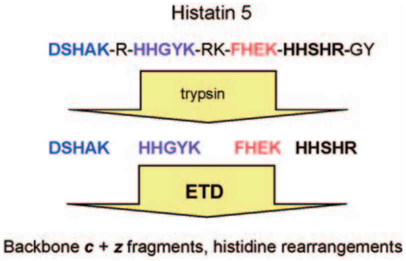

108–113

On the Activation of Chloromethanes by Cyclometalated [Pt(bipy – H)]$^+$ in the Gas Phase: A Mechanistic Study

Burkhard Butschke, Helmut Schwarz

In the ion/molecule reactions of cyclometalated [Pt(bipy – H)]$^+$ with the chloromethanes $CH_{4-n}Cl_n^+$ (n = 1–4) insertion of platinum into the C–Cl bond corresponds to the first step. Next, a 1,2-methyl shift results in C–C bond coupling for substrates with n = 1–3; afterwards, HCl is lost with the hydrogen atom originating from either the incoming substrate or from the (bipy– H) ligand. In the reaction with CH_2Cl_2, the most dominant process corresponds to a CH_2 transfer to the (bipy– H) ligand concomitant with the formation of neutral $PtCl_2$.

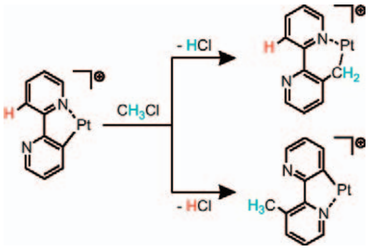

114–122

DC potentials applied to an end-cap electrode of a 3D ion trap for enhanced MS^n functionality

Boone M. Prentice, Wei Xu, Zheng Ouyang, Scott A. McLuckey

▶ The effects of the application of various DC magnitudes and polarities to an end-cap of a 3D quadrupole ion trap throughout a mass spectrometry experiment were investigated. Application of a monopolar DC field was achieved by applying a DC potential to the exit end-cap electrode, while maintaining the entrance end-cap electrode at ground potential. Control over the monopolar DC magnitude and polarity during time periods associated with ion accumulation, mass analysis, ion isolation, ion/ionreaction, and ion activation can have various desirable effects. Included amongst these are increased ion capture efficiency, increased ion ejection efficiency during mass analysis, effective isolation of ions using lower AC resonance ejection amplitudes, improved temporal control of the overlap of oppositely charged ion populations, and the performance of “broad-band” collision induced dissociation (CID). These results suggest general means to improve the performance of the 3D ion trap in a variety of mass spectrometry and tandem mass spectrometry experiments.

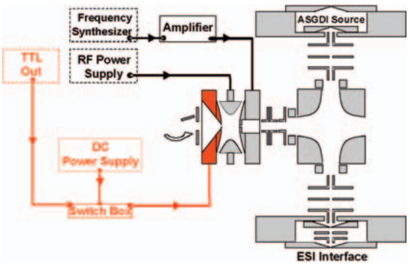

123–128

Electron attachment to $POCl_3$. II. Dependence of the attachment rate coefficients on gas and electron temperature

Nicholas S. Shuman, Thomas M. Miller, Albert A. Viggiano, Jürgen Troe

▶ Electron attachment can be represented by electron capture and electron–phonon coupling.
▶ Elec-tron attachment rate coefficients lead to cross sections and detachment rate constants.
▶ Electron attachment to $POCl_3$ is analyzed in terms of electron-polar neutral capture theory.

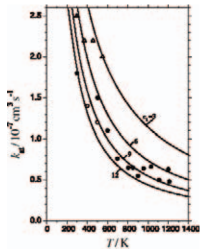

129–137

Mass analyzed threshold ionization (MATI) spectroscopy of trichlorobenzenes via different intermediate vibrational states in the S_1 state

Frank Witte, Mikko Riese, Frank Gunzer, Jürgen Grotemeyer

► Trichlorobenzenes exhibit various vibrational structures in ionic ground state. ► Jahn–Teller effect of 1,3,5-trichlorobenzene investigated. ► Ionization energies of trichlorobenzenes measured.

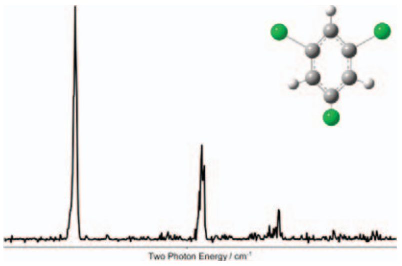

138–149

A mechanistic study of the prominent loss of H_2O from ionized 2-hydroxyaminoethanol

Karl J. Jobst, Shaheda Jogee, Richard D. Bowen, Johan K. Terlouw

► Metastable 2-hydroxyaminoethanol ions abundantly lose water. ► Experiment and theory agree that the elusive 1,2-oxazetidine ion is generated. ► CBS-QB3 model chemistry calculations lead to an intriguing mechanism.

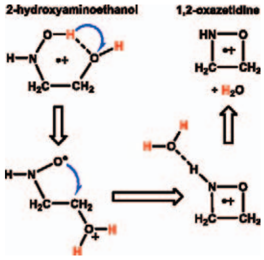

150–158

Implementation of a Penning ionization source on a FTICR instrument with ion funnel optics

Clotilde Le Vot, Carlos Afonso, Claude Beaugrand, Jean-Claude Tabet

► A Penning ionization source was coupled to a FTICR instrument. ► Ion funnels optics have been usedunder low pressure conditions. ► The source is very useful for selective ionization and internal energy control.

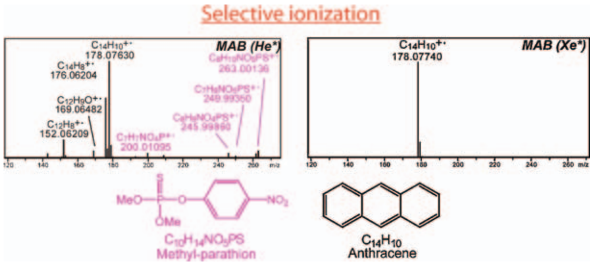

159–166

The role of ion/neutral complexes in the fragmentation of *N*-benzyl-(alkylpyridinium) ions

Dietmar Kuck, Hans-Friedrich Grützmacher, Dieter Barth, Sandra Heitkamp, Matthias C. Letzel

► *N*-benzylpyridinium ions were found to fragment via ion/neutral complexes. ► Alkyl substituents at *the pyridine nucleus* were used as hydride-donor probes. ► Intra-complex H⁻ transfer occurs with *ortho*-isopropyl and -benzyl groups only. ► Reorientation within theI/Ncomplexes is a crucial factor. ► The $C_7H_7^+$ ion leaving the N atom can undergo intra-complex electrophilic attack.

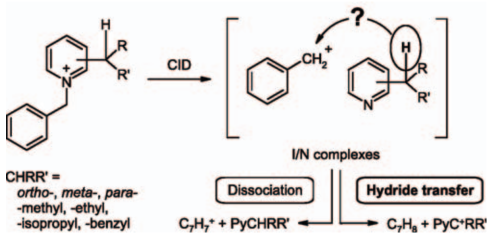

167–174

Isomerization of the constituents of ion/neutral complexes during the fragmentation of protonated dialkyl-substituted 1,3-diphenylpropanes

Dietmar Kuck, Carsten Matthias, Dieter Barth, Matthias C. Letzel

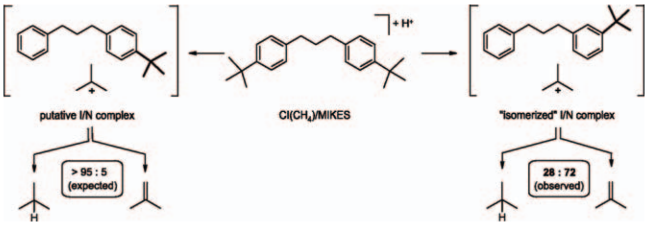

► Isomerization of the neutral constituent of ion/neutral complexes ► Isomerization of the ionic constituent of ion/neutral complexes H$^+$-induced 1,2-*t*-C_4H_9 shift affects the intra-complex reactivity of the neutral ► Cyclohexyl vs. methylcyclopentyl cations as constituents of I/N complexes ► Designed synthesis enables the generation of “tailored” I/N complexes

175–181

The influence of fragment size and intermediate barriers on competing near-identical simple cleavage reactions: A variational RRKM study

Theis I. Sølling, Steen Hammerum, Tore Vulpius

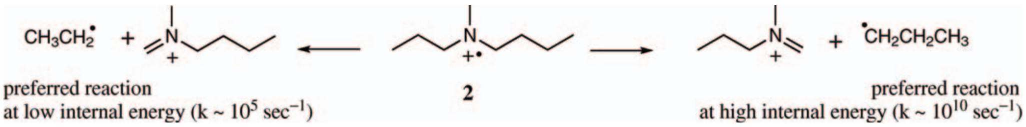

► Fragmentation reactions of almost-symmetrical radical cations exhibit remarkable energy dependent selectivity, which can be accounted for with variational transition state theory. ► Relative rates are not governed by product-like orbiting transition states, but by relatively tight transition states; however, these may not be equally tight. ► The transition states for competing cleavage reactions can exhibit energy-dependent shifting.

182–186

Effect of proline position on symmetric versus asymmetric fragmentation of doubly-protonated tryptic-type peptides

Alex G. Harrison

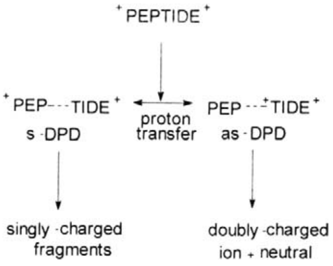

► Tryptic-type peptides undergo symmetric or asymmetric amide bond cleavage. ► Competition between cleavage N-terminal to Pro versus cleavage of second amide bond. ► Position of Pro residue has major effect on fragmentation modes

187–195

Miniature mass spectrometer equipped with electrospray and desorption electrospray ionization for direct analysis of organics from solids and solutions

Ewa Sokol, Robert J. Noll, R. Graham Cooks, Luther W. Beegle, Hugh I. Kim, Isik Kanik

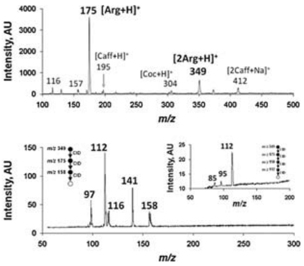

► Small light-weight mass spectrometer (MS) used for chemical analysis of organic material directly from solution or from the solid state. ► Miniature MS performance characterizedby direct analysis of several target compound classes including biotic and abiotic amino acids, purines, pyrimidines, nucleosides and peptides. ► High specificity of the miniature MS system demonstrated using tandem MS and multiple MS stages (up to MS^5). ► Tandem mass spectrometry (MS^2) successfully applied to confirm trace detection of target compounds in mixtures. ► Multiple stage (MS^n) analysis, where n = 3–5, employed for molecular structure confirmation and to demonstrate the high chemical specificity as well as the sensitivityof the instrumentation.

196–203

Two-dimensional FT-ICR/MS with IRMPD as fragmentation mode

Maria A. van Agthoven, Marc-André Delsuc,
Christian Rolando

► 2D FT-ICR/MS adapts to digital instruments with gas-free fragmentation. ► 2D mass spectra show a good correspondence with theory and MS/MS spectra. ► 2D mass spectra of complex samples are sensitive over a large dynamic range. ► Techniques adapted from 2D NMR can turn 2D FT-ICR/MS into a viable analytical tool.

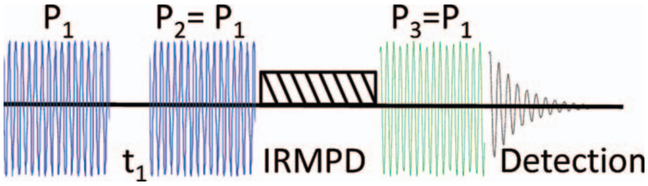

204–209

Interaction of small hydrocarbon ions and Ar⁺ with carbon-fibre-composite surfaces at room temperature

Alan Keim, Bilal Rasul, Nikolaus Endstrasser, Paul Scheier,
Tilmann D. Märk, Zdenek Herman

► Fragmentation on room-temperature CFC surface similar to those on carbon surfaces. ► Surface reactions similar to those on carbon surfaces. ► Increased amounts of K^+ and Na^+ observed (presumably from surface preparation). ► Ar^+ exhibits mostly sputtering of surface material (hydrocarbon ions, K^+, Na^+).

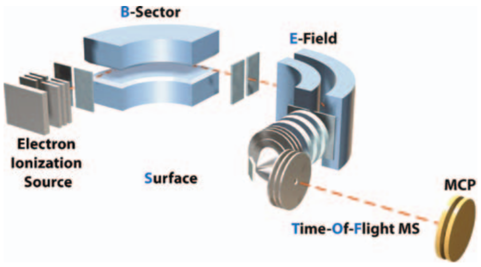

210–218

Thermal decomposition of *t*-amyl methyl ether (TAME) studied by flash pyrolysis/supersonic expansion/vacuum ultraviolet photoionization time-of-flight mass spectrometry

Thomas Hellman Morton, Kevin H. Weber, Jingsong Zhang

► Molecular elimination is the predominant unimolecular dissociation of neutral TAME below 1000 K. ► MeOH elimination from neutral TAME gives 2-methyl-1-butene and 2-methyl-2-butene in a ≈3:1 ratio. ► 118.2 nm photoionization shows that neutral TAME begins to pyrolyze to CH_3 and C_2H_5 radicals >850 K. ► Ketones from successive loss of 2 radicals from neutral TAME are detected at the onset of homolysis. ► Acetone and butanone (ratio ≈2:1) give photoion intensities less than those of C_2H_5 or CH_3 radicals.

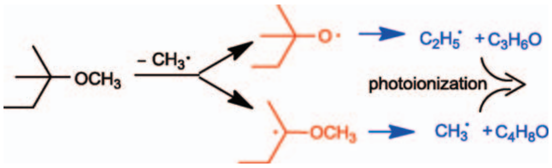

219–226

Sequential IRMPD of $XGe(OEt)_4^-$ ions: Gas-phase synthesis of novel oxy-germanium anions

Luciano A. Xavier, Thaciana V. Malaspina, Nelson H. Morgon,
Jair J. Menegon, José M. Riveros

► Gas-phase F^- ions react readily with $Ge(OEt)_4$ to yield the hypervalent $FGe(OEt)_4^-$. ► $FGe(OEt)_4^-$ undergoes facile IRMPD through three different channels. ► Sequential IRMPD processes are observed for the primary IRMPD products. ► Isomeric germanate and germyl anions can be distinguished by their proton affinity. ► IRMPD allows for the gas-phase synthesis of novel oxy-germanium ions.

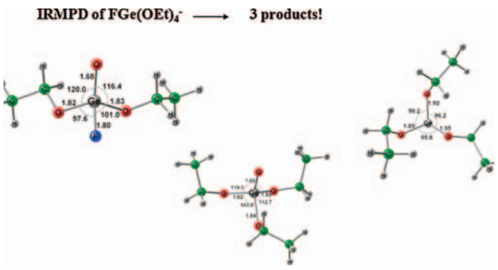

227–231

Towards data acquisition throughput increase in Fourier transform mass spectrometry of proteins using double frequency measurements

Aleksey Vorobyev, Mikhail V. Gorshkov, Yury O. Tsybin

▶ Double frequency detection in FT-ICRMS applied to proteins. ▶ Increased FT-ICR MS data acquisition throughput for proteins. ▶ Confirmation of multiple frequency potential for FT-ICR MS advancement.

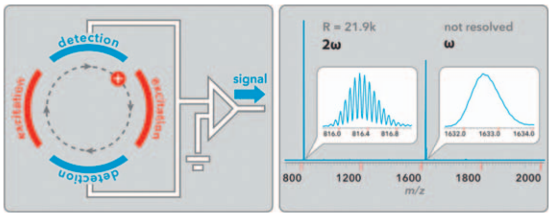

232–240

Deprotonated *N*-(2,4-dinitrophenyl)amino acids undergo cyclization in solution and the gas phase

M. George, V. Ramesh, R. Srinivas,
Daryl Giblin, Michael L. Gross

▶ [M−H]⁻ of title compounds dissociate via sequential eliminations of CO_2 and H_2O. ▶ Products of dissociation are cyclized deprotonated benzimidazole-*N*-oxide derivatives. ▶ Structures determined by MS/MS, synthesis of reference compounds, and theory. ▶ Gas-phase cyclization is analog of the base-catalyzed solution reaction.

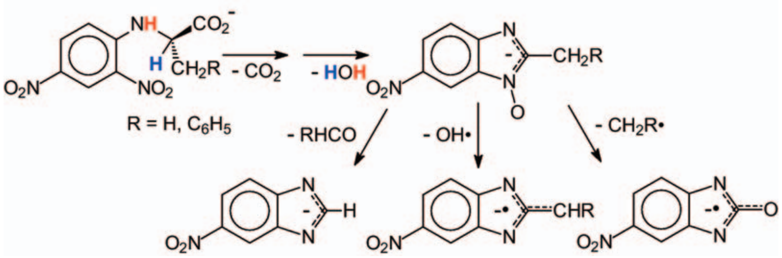

241–245

Absorption of the green fluorescent protein chromophore anion in the gas phase studied by a combination of FTICR mass spectrometry with laser-induced photodissociation spectroscopy

Konstantin Chingin, Roman M. Balabin, Vladimir Frankevich,
Konstantin Barylyuk, Robert Nieckarz, Pavel Sagulenko,
Renato Zenobi

▶ Optical absorption of the green fluorescent protein chromophore anion ($HBDI^-$) in the gas phase was probed by photo-induced dissociation ("action") spectroscopy. ▶ A pronounced dependence on the laser irradiance was found ▶ Dissociation at high irradiance is governed by multiple-photon absorption processes whose efficiency peaks between 476 and 488 nm. ▶ At very low irradiance (<0.4 m Wcm^{-2}) dissociation of gas-phase $HBDI^-$ is mostly promoted by single-photon transitions. ▶ The intrinsic absorption maximum of gas-phase $HBDI^-$ <476 nm is thus suggested to be blue-shifted compared to earlier results obtained with pulsed lasers.

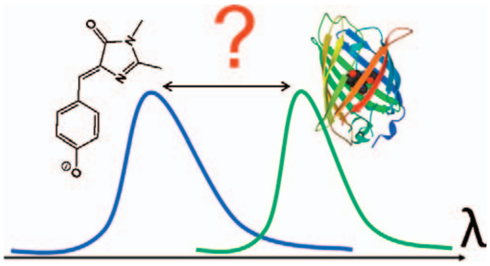

246–252

Predator data station: A fast data acquisition system for advanced FT-ICR MS experiments

Greg T. Blakney, Christopher L. Hendrickson, Alan G. Marshall

▶ We describe hardware and software to control FT-ICR MS experiments. ▶ Our data station controls excitation and detection of a time-domain ICR signal. ▶ We achieve mass resolving power of 20,000 for ion selection.